An efficient domain decomposition method with cross-point treatment for Helmholtz problems

Axel Modave, Xavier Antoine, Christophe Geuzaine

CSMA 2019
14ème Colloque National en Calcul des Structures
13-17 Mai 2019, Presqu'île de Giens (Var)

An efficient domain decomposition method with cross-point treatment for Helmholtz problems

A. Modave [1], X. Antoine [2], C. Geuzaine [3]

[1] *POEMS, CNRS-ENSTA-Inria, Palaiseau (France),* axel.modave@ensta-paristech.fr
[2] *Université de Lorraine, CNRS, Inria, IECL (France),* xavier.antoine@univ-lorraine.fr
[3] *Université de Liège (Belgium),* christophe.geuzaine@uliege.be

Abstract — The parallel finite-element solution of large-scale time-harmonic scattering problems is addressed with a non-overlapping domain decomposition method. The efficiency of this method strongly depends on the transmission condition enforced on the interfaces between the subdomains. Conditions based on high-order local absorbing boundary conditions have proved well suited for configurations without cross points (*i.e.* points where more than two subdomains meet). In this work, we extend this approach to efficiently deal with cross points. Two-dimensional numerical results are presented.
Mots clés — propagation des ondes, équation de Helmholtz, éléments finis, calcul parallèle

1 Introduction

Solving high-frequency time-harmonic scattering problems using finite element techniques is challenging, as such problems lead to very large, complex and indefinite linear systems. Optimized Schwarz domain decomposition methods (DDMs) are currently a very promising approach, where subproblems of smaller sizes are solved in parallel using direct solvers, and are combined in an iterative procedure.

It is well-known that the convergence rate of these methods strongly depends on the transmission condition enforced on the interfaces between the subdomains. Local transmission conditions based on high-order absorbing boundary conditions (HABCs) have proved well suited [1, 2]. They represent a good compromise between basic impedance conditions (which lead to suboptimal convergence) and the exact Dirichlet-to-Neumann (DtN) map related to the complementary of the subdomain (which is expensive to compute). However, a direct application of this approach for domain decomposition configurations with cross-points, where more than two subdomains meet, does not provide satisfactory results.

We present an improved DDM that efficiently addresses configurations with cross points. Noting that these points actually are corners for the subdomains, our strategy consists in incorporating a corner treatment developed for HABCs into the DDM procedure. After a presentation of the key aspects of the methods, the effectiveness of our approach is discussed with two-dimensional finite element results.

2 Helmholtz problem with HABC and corner treatment

In order to solve scattering problems set on infinite or very large domains by finite element methods, a common strategy consists in computing the numerical solution only on a truncated computational domain, and using a non-reflecting treatment at the artificial boundary, such as a HABC or a perfectly matched layer (PML). To describe our approach, we consider a two-dimensional Helmholtz problem defined on a rectangular computational domain Ω:

$$\begin{cases} \Delta u + k^2 u = s, & \text{in } \Omega, \\ \partial_{n_f} u + \mathcal{B} u = 0, & \text{on } \Gamma_f, \quad (f = 1 \dots 4) \end{cases} \tag{1}$$

where $k(\mathbf{x})$ is the wavenumber, $s(\mathbf{x})$ is a source term, Γ_f is an edge of the rectangular domain, ∂_{n_f} is the exterior normal derivative on $\Gamma_f \subset \partial\Omega$, and $\mathcal{B}$ is a non-reflecting boundary operator. Following [3], we use a Padé-type HABC, which is obtained by approximating to exact DtN operator for the half-space

problem, with constant k and $s = 0$ outside. It corresponds to using, for each edge Γ_f,

$$\mathcal{B}u = -\imath k\alpha u - \frac{2\imath\alpha k}{M}\sum_{i=1}^{N} c_i(u_{f,i}+u), \quad \text{on } \Gamma_f,$$

and introducing N auxiliary fields $\{u_{f,i}\}_{i=1}^{N}$ governed by the auxiliary equations

$$\partial^2_{\tau\tau}u_{f,i} + k^2\big((\alpha^2 c_i+1)u_{f,i} + \alpha^2(c_i+1)u\big) = 0, \quad \text{on } \Gamma_f, \quad (i = 1\dots N) \tag{2}$$

where $\partial^2_{\tau\tau}$ is the second-order tangent derivative, $\alpha = e^{\imath\phi/2}$, $c_i = \tan^2(i\pi/M)$ and $M = 2N+1$. The accuracy of the numerical solution at the boundary depends on the number N and the angle ϕ [3].

Because of the spatial derivative in equation (2), additional boundary conditions must be prescribed on the auxiliary fields at the boundary of the edges (*i.e.* at the corner of the domain) to close the system. Following [4, 5], we introduce new relations that ensure the compatibility of the system without any supplementary approximation. With these relations, the auxiliary fields defined on adjacent edges are coupled at the common corner. For the fields $\{u_{f,i}\}_{i=1}^{N}$ defined on Γ_f, having an adjacent edge $\Gamma_{f'}$, the boundary conditions at the corner $P_{f,c} = \Gamma_f \cap \Gamma_{f'}$ can be written as

$$\partial_{n_{f,c}}u_{f,i} + \mathcal{D}u_{f,i} = 0, \quad \text{on } P_{f,c}, \quad (i = 1\dots N) \tag{3}$$

with

$$\mathcal{D}u_{f,i} = -\imath k\alpha u_{f,i} - \frac{2\imath\alpha k}{M}\sum_{j=1}^{N} c_j \frac{(\alpha^2 c_i + 1 - \alpha^2)u_{f,i} - \alpha^2(c_i+1)u_{f',j}}{\alpha^2 c_i + \alpha^2 c_j + 1} = 0, \quad \text{on } P_{f,c}, \quad (i = 1\dots N)$$

where $\partial_{n_{f,c}}$ is the exterior normal derivative at $P_{f,c} \subset \partial\Gamma_f$, and $\{u_{f',j}\}_{j=1}^{N}$ are the auxiliary fields defined on $\Gamma_{f'}$. Finally, the problem consists in solving the main field $u(\mathbf{x})$ on the domain with boundary conditions on the edges (equation (1)) and N auxiliary fields on each edge with boundary conditions at the corners (equations (2)-(3)). See [4] for a three-dimensional version of this strategy.

3 A non-overlapping DDM with cross-point treatment

The Helmholtz problem defined on Ω is decomposed into subproblems defined on non-overlapping subdomains Ω_I $(I = 1\dots N^{\text{dom}})$, with $\Omega = \overline{\bigcup_I \Omega_I}$ and $\Omega_I \bigcap \Omega_J = \emptyset$ if $I \neq J$. We consider here a structured decomposition of a rectangular domain Ω into an array of rectangular subdomains (see figure 1). The edges of each subdomain Ω_I are denoted $\Gamma_{I,f}$ $(f = 1\dots 4)$. Each edge could be an *interface edge* (if there is a neighboring subdomain beyond the edge) or a *boundary edge* (if it belongs to the boundary of Ω).

At each iteration of the DDM algorithm, the subproblems are solved in parallel, and data are exchanged at the interfaces between the subdomains to synchronize the solutions. The additive Schwarz DDM can be described as follows, at iteration $\ell+1$:

- For all subdomain Ω_I, compute $u_I^{\ell+1}$ solution to

$$\begin{cases} \Delta u_I^{\ell+1} + k^2 u_I^{\ell+1} = s, & \text{in } \Omega_I, \\ \partial_{n_{I,f}} u_I^{\ell+1} + \mathcal{B}u_I^{\ell+1} = g_{I,f}^{\ell}, & \text{on } \Gamma_{I,f}, \quad (f = 1\dots 4) \end{cases}$$

  where $g_{I,f}^{\ell}$ is a transmission variable if $\Gamma_{I,f}$ is an interface edge, or it is set to zero if $\Gamma_{I,f}$ is a boundary edge.

- For all interface between neighboring subdomains Ω_I and Ω_J, update the transmission variables $g_{I,f}^{\ell+1}$ and $g_{J,g}^{\ell+1}$ according to

$$\begin{aligned} g_{I,f}^{\ell+1} &= -g_{J,g}^{\ell} + 2\mathcal{B}u_J^{\ell+1}, \quad \text{on } \Gamma_{J,g}, \\ g_{J,g}^{\ell+1} &= -g_{I,f}^{\ell} + 2\mathcal{B}u_I^{\ell+1}, \quad \text{on } \Gamma_{I,f}, \end{aligned}$$

  where $\Gamma_{I,f} = \Gamma_{J,g}$ is the common interface edge.

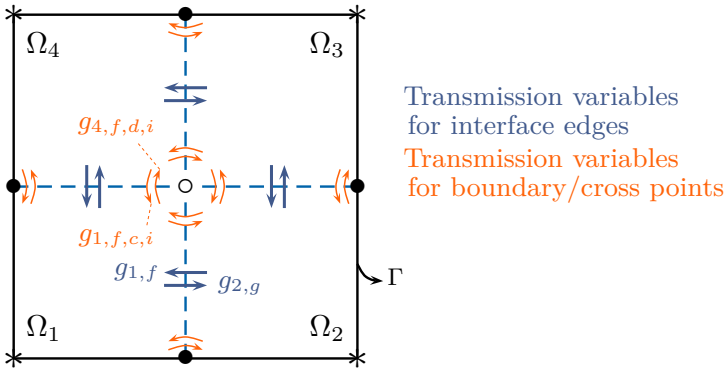

Figure 1: Example of domain decomposition (2×2 configuration) with the transmission variables.

The convergence of this algorithm is accelerated by using an iterative Krylov method (GMRES) on the top of the procedure for updating the transmission variables. See *e.g.* [1] for more details.

Because the HABC is used as transmission operator (on the interface edges) and as boundary operator (on the boundary edges), the description of the DDM algorithm is incomplete. It should include the auxiliary fields defined on the edges and, since these fields are governed by equation (2), additional conditions should be prescribed at the boundary of the edges. The boundary points of each edge $\Gamma_{I,f}$ are denoted $P_{I,f,c}$ ($c = 1,2$). Each point could be a *cross point* (at the cross of two interface edges), a *corner point* (at the cross of two boundary edges) or a *boundary point* (at the cross of one interface edge and one boundary edge). They are represented with the symbols $\circ$, $\bullet$ and $*$ on figure 1.
At iteration $\ell+1$ of the DDM algorithm, we have the additional operations:

- For all boundary/interface edge $\Gamma_{I,f}$, compute the auxiliary field $u_{I,f,i}^{\ell+1}$ solution to

$$\begin{cases} \partial_{\tau\tau}^2 u_{I,f,i}^{\ell+1} + k^2\big((\alpha^2 c_i + 1)u_{I,f,i}^{\ell+1} + \alpha^2(c_i+1)u_I^{\ell+1}\big) = 0, & \text{on } \Gamma_{I,f}, \\ \partial_{n_{I,f,c}} u_{I,f,i}^{\ell+1} + \mathcal{D}u_{I,f,i}^{\ell+1} = g_{I,f,c,i}^{\ell}, & \text{at } P_{I,f,c}, \quad (c=1,2) \end{cases}$$

  where $g_{I,f,c,i}^{\ell}$ is a transmission variable if the adjacent edge of $\Gamma_{I,f}$ at the boundary point $P_{I,f,c}$ is an interface edge, or it is set to zero if the adjacent edge is a boundary edge.

- For all boundary/cross point shared by the edges $\Gamma_{I,f}$ and $\Gamma_{J,f}$ of neighboring subdomains Ω_I and Ω_J, update the transmission variables $g_{I,f,c,i}^{\ell}$ and $g_{J,f,d,i}^{\ell}$ according to:

$$\begin{aligned} g_{I,f,c,i}^{\ell+1} &= -g_{J,f,d,i}^{\ell} + 2\mathcal{D}u_{J,f,i}^{\ell+1}, \quad \text{on } P_{J,f,d}, \\ g_{J,f,d,i}^{\ell+1} &= -g_{I,f,c,i}^{\ell} + 2\mathcal{D}u_{I,f,i}^{\ell+1}, \quad \text{on } P_{I,f,c}, \end{aligned}$$

  where $P_{I,f,c} = P_{J,f,d}$ is the common point.

The auxiliary fields of two adjacent edges of one subdomain are coupled by the operator $\mathcal{D}$ at the common corner. All these operations are rather naturally included in the DDM algorithm. A GMRES is used for updating all the transmission variables, which are now associated to shared edges and shared points.

4 Finite element results

In order to verify and to analyze the efficiency of the proposed DDM, we present finite element results obtained with two 2D benchmarks. The numerical scheme is based on a Galerkin method adapted from [1], with meshes made of triangles, nodal finite elements, and linear basis functions. The simulations are made with the `GetDP` and `GetDDM` environments [6].

4.1 Benchmark 1 — Scattering of a plane wave by a sound-soft circular cylinder

We consider the scattering of an incident plane wave by a disk. The scattered field is computed on a rectangular domain Ω, which is partitioned into six subdomains (figure 2). A Neumann condition is

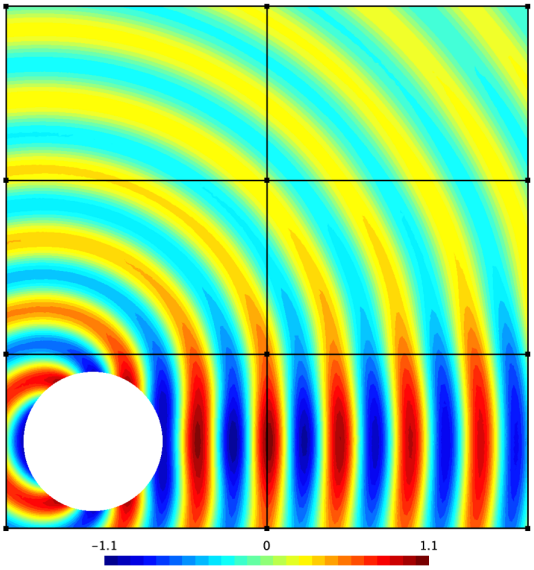

Figure 2: Scattering benchmark: Configuration and solution.

(a) Relative residual

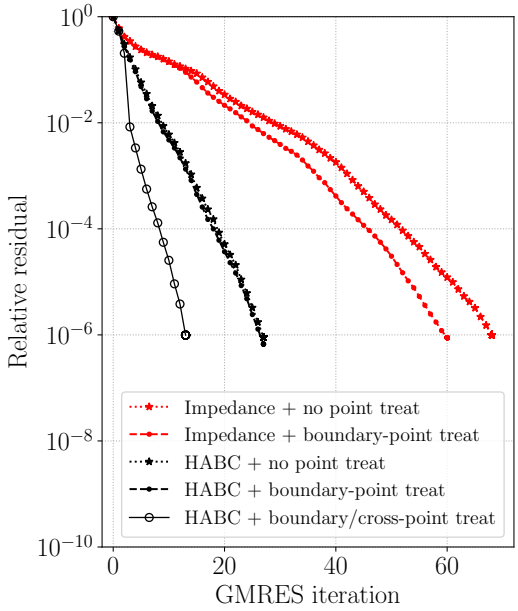

(b) Relative L^2-error

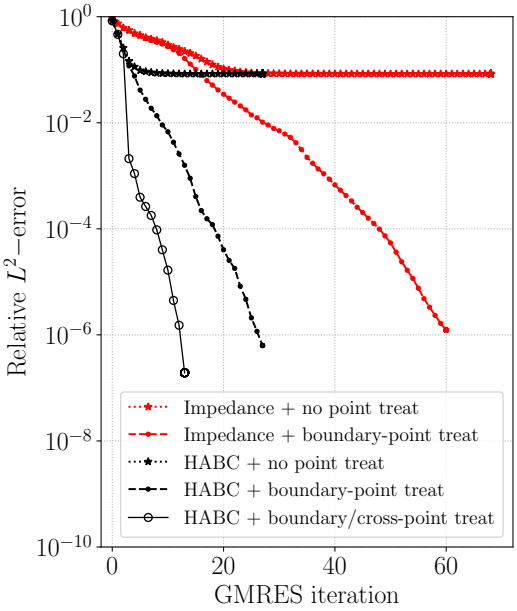

Figure 3: Scattering benchmark: History of residual (a) and L^2-error between the DDM solution and the monodomain numerical solution (b). The transmission operators are based on the basic impedance condition (red lines) or the HABC (black lines), with and without boundary/cross-point treatments. Parameters: $N = 4$ and $\phi = \pi/3$

prescribed on the boundary of the disk, and the HABC with the corner treatment is used on the exterior boundary. In the DDM algorithm, transmission operators based on an optimized impedance condition [2] and the HABC are tested. In the former case, a specific treatment ensures the compatibility between the impedance condition (on the interface edges) and the HABC (on the boundary edges) at the boundary points. The effect of the boundary/cross-point treatments is analyzed by keeping or removing the corresponding terms in the finite element scheme.

For both kinds of transmission operator, the boundary-point treatment is required for converging towards the good solution. Indeed, without this treatment, the residual decreases with the iteration number, but the error stagnates (figure 3). By contrast, the error decreases correctly when the boundary-point treatment is enabled. In that case, the convergence is faster with the transmission operator based on the HABC, and it is even faster with the cross-point treatment.

4.2 Benchmark 2 — Marmousi case with heterogeneous medium

We finally address a more challenging benchmark with a heterogeneous medium: the Marmousi model, which represents a realistic geological structure (figure 4). Although the HABC was initially derived by assuming a constant wavenumber, it provides good accuracy for problems with heterogeneous media [4], and we observe that it accelerates the convergence of the DDM for the Marmousi benchmark (figure 5).

On figure 6, the convergence of the method is compared for different domain partitions. For a larger number of subdomains (which is required to solve large problems), the DDM converges significantly faster with a multi-dimensional partition than with the mono-dimensional partition, which confirms the efficiency and the interest of our approach.

(a) Velocity model

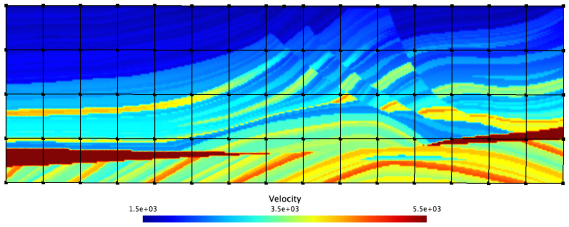

(b) Reference numerical solution u_{red}

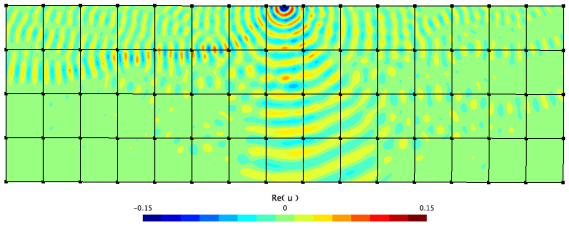

Figure 4: Marmousi benchmark: Velocity model (a) and reference numerical solution (b). The HABC is used as boundary condition.

(a) Relative residual

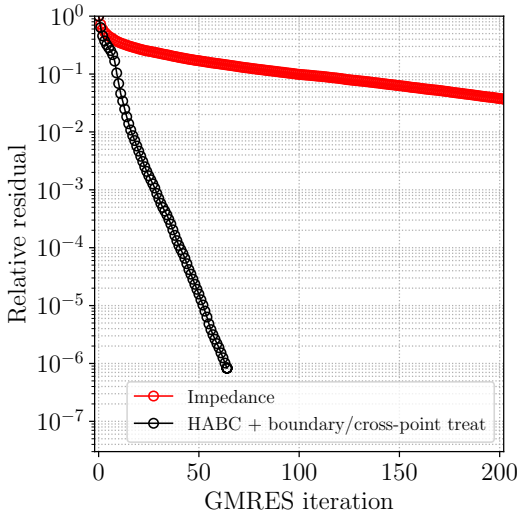

(b) Relative L^2-error

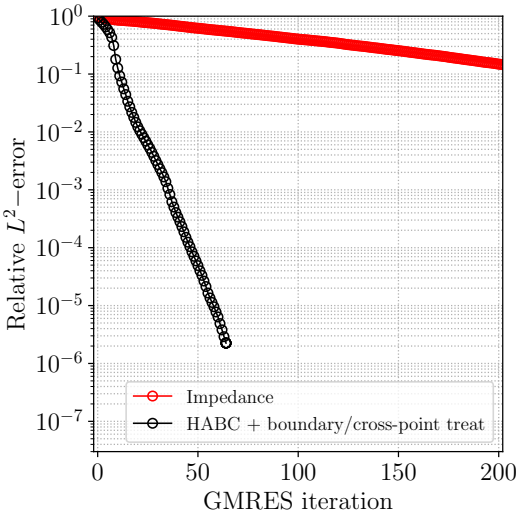

Figure 5: Marmousi benchmark: History of residual (a) and L^2-error (b) for transmission operators based on the basic impedance condition (red lines) or the HABC (black lines) with point treatments. Parameters: $N = 4$ and $\phi = \pi/3$

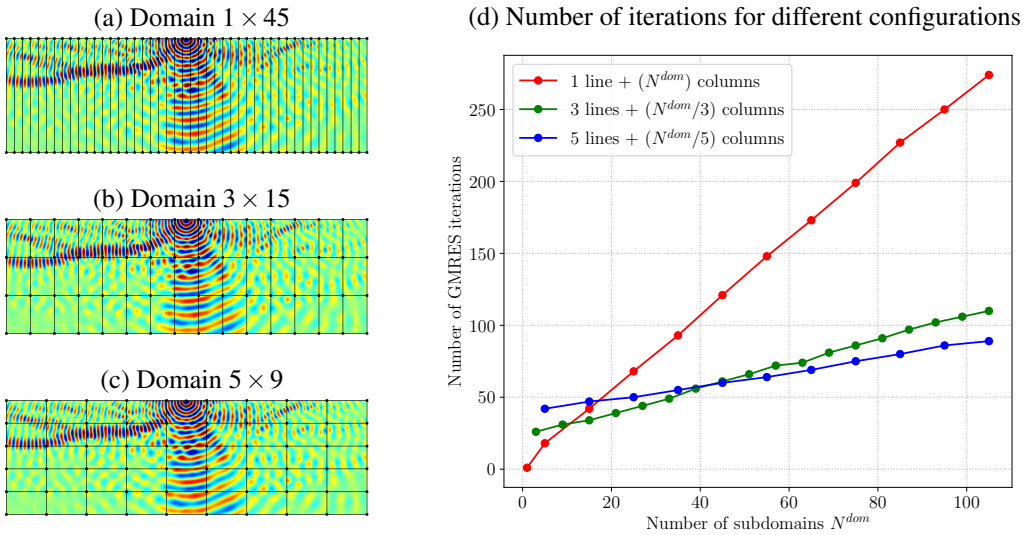

Figure 6: Marmousi benchmark: Three kinds of domain partition (a)-(c). The HABC is used both as boundary condition and transmission operator. The point treatments are enabled. The number of iterations to reach the relative residual 10^{-6} is plotted as a function of the number of subdomains for the three kinds of domain partition (d).

References

[1] Y. Boubendir, X. Antoine, C. Geuzaine. *A quasi-optimal non-overlapping domain decomposition algorithm for the Helmholtz equation*, Journal of Computational Physics 231 (2), 262–280, 2012

[2] M. Gander, F. Magoules, F. Nataf. *Optimized Schwarz methods without overlap for the Helmholtz equation*, SIAM Journal on Scientific Computing 24 (1), 38–60, 2002

[3] R. Kechroud, X. Antoine, A. Soulaïmani. *Numerical accuracy of a Padé-type non-reflecting boundary condition for the finite element solution of acoustic scattering problems at high-frequency*, International Journal for Numerical Methods in Engineering 64 (10), 1275–1302, 2005

[4] A. Modave, A. Atle, J. Chan, T. Warburton. *A GPU-accelerated nodal discontinuous Galerkin method with high-order absorbing boundary conditions and corner/edge compatibility*, International Journal for Numerical Methods in Engineering 112 (11), 1659–1686, 2017

[5] A. Modave, C. Geuzaine, X. Antoine. *Corner treatment for high-order local absorbing boundary conditions in high-frequency acoustic scattering*, Submitted, 2018

[6] B. Thierry, A. Vion, S. Tournier, M. El Bouajaji, D. Colignon, N. Marsic, X. Antoine, C. Geuzaine. *GetDDM: an open framework for testing optimized Schwarz methods for time-harmonic wave problems*, Computer Physics Communications 203, 309–330, 2016